Parallel large-eddy simulations of turbulent flows with complex moving boundaries on fixed Cartesian grids

Jianming Yang [a] and Elias Balaras [a] *

[a]Department of Mechanical Engineering, University of Maryland,
College Park, MD 20742, USA

A parallel embedded boundary approach for large-eddy simulations of turbulent flows with complex geometries and dynamically moving boundaries on fixed orthogonal grids is presented. The underlying solver is based on a second-order fractional step method on a staggered grid. The boundary conditions on an arbitrary immersed interface are satisfied via second-order local reconstructions. The parallelization is implemented via a slab decomposition. Several examples including laminar flow past a sphere up to $Re = 300$, transitional flow past an airfoil at $Re = 10,000$, and turbulent flow over a traveling wavy wall at $Re = 10,170$ are presented to establish the accuracy and performance of the method.

1. INTRODUCTION

Today with the advent of inexpensive parallel computers state-of-the-art modeling strategies for simulating turbulent and transitional flows -i.e. direct numerical simulations (DNS) and large-eddy simulations (LES)- are continuously expanding into new areas of applications. Particularly attractive examples, from the perspective of the required spatio-temporal resolution, are from the field of medicine and biology, where in most cases transitional and low Reynolds numbers flows are of interest. The challenge in this case, however, is to properly account for the complex fluid-structure interactions that dominate the dynamics of these flows. The use of numerical methods based on unstructured grids is a possibility, but usually the transition to parallel platforms is fairly complex. Mesh partition, load balance, and the inversion of large sparce matrixes are the most commonly encountered bottlenecks in efficient parallelization. Furthermore, in most cases the intrinsic dissipative discretizations make them problematic in DNS and LES.

The use of embedded boundary formulations, where a complex moving boundary can be modeled on a structured Cartesian grid is an attractive strategy especially for problems with boundaries undergoing large motions/deformations. A basic advantage of this strategy is that highly efficient and energy conserving numerical methods can be used. In addition, their implementation on parallel platforms is usually fairly straightforward. In the this paper we will present an efficient, parallel, embedded boundary formulation applicable LES of complex external flows. In the next section the numerical method and

*Financial support from the National Institutes of Health (Grant R01-HL-07262) and the National Science Foundation (Grant CTS-0347011) is gratefully acknowledged.

parallelization strategy will be briefly described. Then, some preliminary results demonstrating the efficiency and range of applicability of the approach will be given.

2. METHODOLOGY

In the LES approach the resolved, large-scale, field is obtained from the solution of the filtered Navier-Stokes equations, where the effect of the unresolved scales is modeled. In the present method, a top-hat filter in physical space is implicitly applied by the finite-difference operators. The resulting subgrid scale (SGS) stresses are modeled using the Lagrangian dynamic SGS model [3]. The filtered equations are discretized using second-order central difference scheme on a staggered grid. Time advancement is done using a fractional-step method, with a second-order Crank-Nicolson scheme for the diffusive terms and a low-storage third-order Runge-Kutta scheme for the convective terms. Both Cartesian and cylindrical coordinate grids can be used.

To compute the flow around complex objects, which are not aligned with the Cartesian grid we have developed a methodology that practically reconstructs the solution in the vicinity of the body according to the target boundary values [1,7]. The approach allows for a precise imposition of the boundary conditions without compromising the accuracy and efficiency of the Cartesian solver. In particular, an immersed boundary of arbitrary shape is identified by a series of material-fixed interfacial markers whose location is defined in the reference configuration of the solid (see Fig. 1). This information is then used to identify the Eulerian grid nodes involved in the reconstruction of the solution near the boundary in a way that the desired boundary conditions for the fluid are satisfied to the desired order of accuracy. The reconstruction is performed around the points in the fluid phase closest to the solid boundary (all points that have least one neighbor in the solid phase). An advantage of this choice is that it simplifies the treatment of the points that emerge from the solid as the boundary moves through the fixed grid. In Fig. 1a, an example of one scheme implementation in [1] is presented, where the solution at each boundary point, is reconstructed along the line normal to the boundary by means of linear interpolation.

3. PARALLELIZATION

The parallelization is implemented via slab decomposition and the parallel communication between among blocks is done using the MPI library. To minimize the communications at the block (slab) interface, the decomposition is carried out in the direction with the largest number of points (usually the streamwise direction). Each block is equally sized, which greatly simplies the mesh partition and provides optimal load balance. Minor modifications are introduced to the original serial solver, as ghost cells at the block interfaces are utilized to provide information from neighboring blocks. In the current implementation, only one layer of ghost cells from the neighboring block are required as the standard second-order central difference scheme is used for the spatial discretization.

Usually the solution of the pressure Poisson equation is the most expensive part of a Navier-Stokes solver, and the parallelization via domain decomposition adds further complications. In the present study, the computational grid is always uniform in spanwise direction; thus the fast Fourier transformation (FFT) can be applied to the Poisson

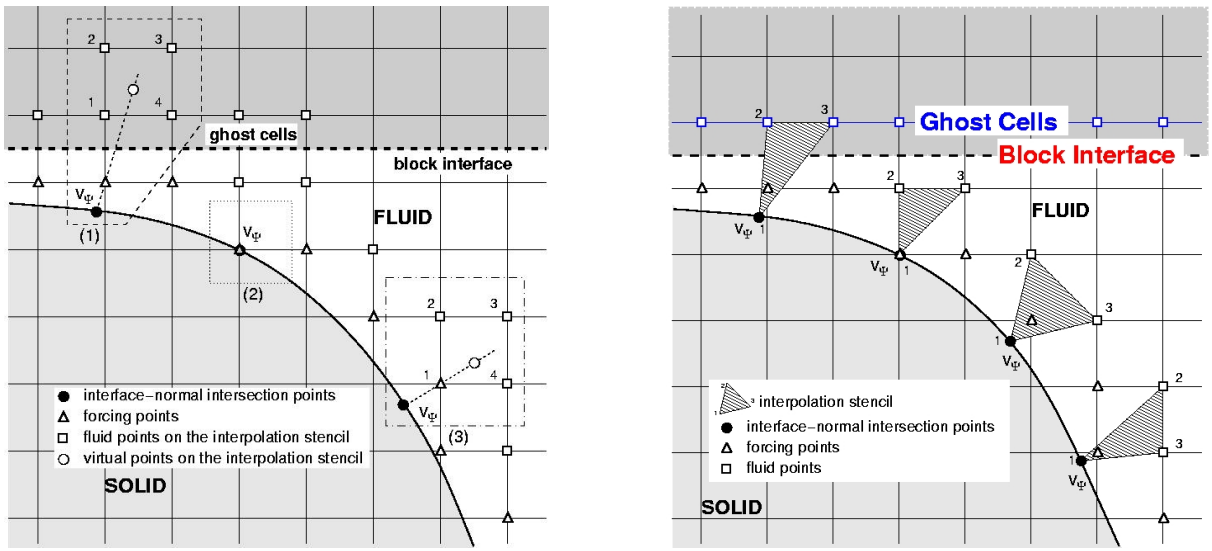

(a) (b)

Figure 1. (a) Interpolation stencil in [1]. (1)-(3) illustrate three possible choices depending on the interface topology and local grid size. One situation when the compuational domain is decomposited in parallel computing in [1]; (b) Interpolation stencil in present approach.

equation in spanwise direction and a series of decoupled two-dimensional problems are obtained and solved using the direct solver from FISHPACK [5]. The FFT is performed in each block and no information from neighboring blocks is required. However, global communication is required to swap the slabs in streamwise direction into slabs in wavenumber space, and swap back after the direct solution of the twodimensional problem for each wavenumber. Nevertheless, the overhead for the global communication is small and, as shown in results part, the speedup for the problem considered is linear.

The interpolation stencil in [1], as shown in Fig. 1a, may contain grid points that do not belong to the neighboring grid lines of the forcing point considered. When domain decomposition is employed in parallel computing, neighboring block should provide boundary conditions to the current block. But the example case requires extra information from the neighboring block. Of course, the information can be provided through extra communication, but the structure of the variable arrays will be modified. To avoid the extra communication and the modification of the variable arrays, one should not involve any points in the interpolation stencil except those on the neighboring grid lines. And while one examine the case in Fig. 1a, it is apparent that points 2 and 3 can be discarded as the intersection point of the line normal to the interface and the grid line through points 1 and 4 can be chosen as the virtual points in case (1) of Fig. 1a. Furthermore, the intersection point of the normal and the diagonal line through points 2 and 4 in case (3) can also act as virtual point. This way, a small stencil as shown in Fig. 1b can be obtained without the extra communication cost might be involved in [1] for parallel computing. This method has been proven to be sucessful for parallel computing.

4. RESULTS

4.1. Simulations of flows with stationary bodies

4.1.1. Flow past a sphere

To validate the accuracy of our method, the laminar flow past a sphere from $Re = 50$ to 1000 is simulated. Cylindrical coordinates are used to take advantadge of the geometry. The flow is steady and axisymmetric for Reynolds number up to 200. While the axisymmetry is broken down and the wake is dominated by periodic vortex shedding. On a grid of $384\times64\times96$ (streamwise $\times$ azimuthol $\times$ radial direction) points, the predicted mean drag and lift coefficients are $C_D = 0.655$ and $C_L = 0.064$, respectively, which are within 1% to the values reported in [2], in which a body-fitted method was adopted. The parallel speedup for this simulation is shown in Fig. 2. Linear speedup is obtained up to 16 processors, which was the limit of the cluster where the preliminary testes were carried out.

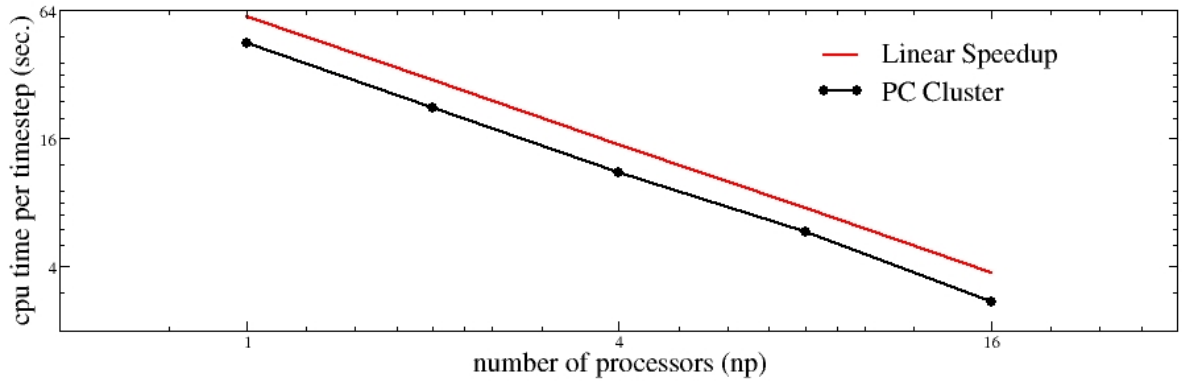

Figure 2. Parallel Speedup for a $384 \times 64 \times 96$ Grid.

A direct numerical simulation of the transitional flow past a sphere at $Re = 1000$ was performed on a grid with nearly 15 million points. At this Reynolds number, small scales are present in the wake and the flow becomes chaotic further downstream. Those small scale structures are generated by the breakdown of the large cylindrical vortical structure enveloping the sphere. The meachanism of this breakdown is due to a Kelvin-Helmholtz-like instability of the shear layer developed from the boundary layer separation of the sphere. In Fig. 3, the instantaneous vortical structures and the azimuthal vorticity contours are shown. The roll-up of the shear layer, the development of large hairpin structures, and the breakdown of larger structures into smaller scales can be clearly observed. The flow becomes turbulent in the far wake. Those results are in very good agreement with the DNS using a high-order spectral method in [6] qualitatively, although the detailed quanitative comparison is to be conducted.

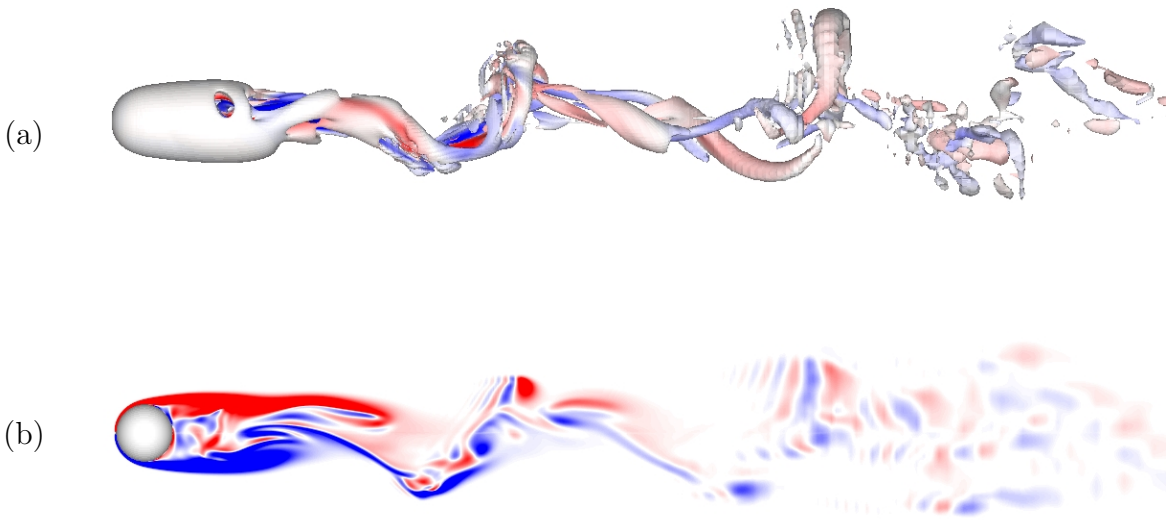

Figure 3. Transitional flow past a sphere at $Re = 1000$. (a) Instantaneous vortical structures visualized using isosurfaces of $Q = 0.1$ colored by the streamwise vorticity; (b) Instantaneous azimuthal vorticity contours.

4.1.2. Transitional flow past an airfoil

A more challenging test-case is the computation of transitional flow around an Eppler E387 airfoil. The angle of attack is 10° and the cord Reynolds number $10,000$. The Reynolds number regime is characteristic of bird flight. LES have been performed on a grid with approximately 18×10^6 nodes ($672 \times 48 \times 560$). The flow field is characterized by the massive separation as shown in Fig. 6 where the mean streamlines are shown. Fig. 5 shows the vortical structures behind the airfoil.

4.2. Simulations of flows with complex moving boundaries

4.2.1. Turbulent flow over a traveling wavy wall

In this section LES of turbulent flow over a flexible wavy wall undergoing transverse motion in a form of streamwise traveling wave is presented. The immersed boundary in this case no longer belongs to a rigid body, but it has a non-uniform prescribed velocity varying with time. Nevertheless, given the availability of accurate DNS data in the literature[4], we can use it to test the accuracy and efficiency of the proposed algorithm in turbulent flows. The parametric space and computational box in these LES are the same as in the reference DNS by Shen et al. [4], where the location of the wall boundary as a function of time is given by $y_w(t) = a \sin k(x - ct)$ (a is the magnitude of the oscillation, $k = 2\pi/\lambda$ is the wavenumber with λ the wavelength, and c is the phase-speed of the traveling wave). We have considered the same wave steepness, $ka = 0.25$, and Reynolds number, $Re = U\lambda/\nu = 10,170$ (U is the mean freestream velocity),A grid of $288 \times 88 \times 64$ (streamwise, vertical, and spanwise direction, respectively) is used here for all the sim-

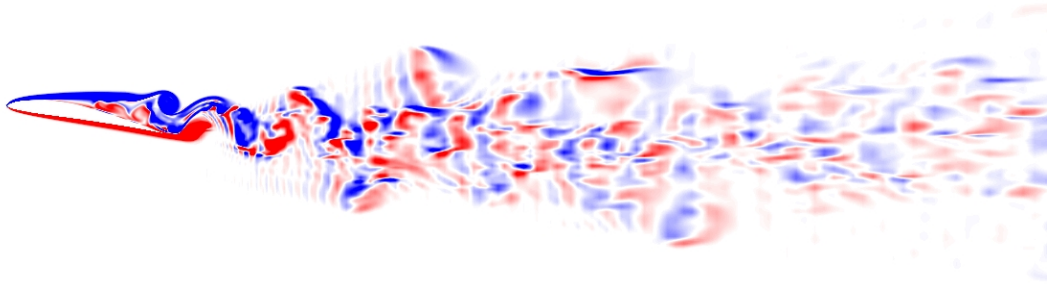

Figure 4. Instantaneous spanwise vorticity contours an E387 airfoil at attack angle 10° for $Re = 10,000$.

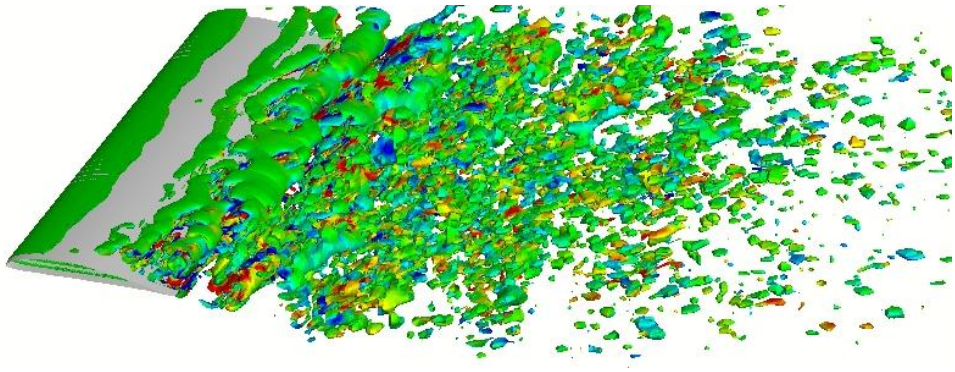

Figure 5. Instantaneous vortical structure.

ulations. The grid is uniform in the streamwise and spanwise homogeneous directions, and is stretched in the vertical direction. In Fig. 7 the instantaneous vortical structures visualized using isosurfaces of the second invariant of the velocity gradient tensor, Q, are shown for $c/U = 0.0$ and c/U = 0.4 (c/U is the ratio of the wave speed to the freestream velocity). It can be seen that the strong streamwise vortices that are characteristic of stationary wavy walls ($c/U = 0$) are suppressed as c/U increased from 0.0 to 0.4. Similar behavior has been observed in the reference DNS [4]. Quantitative comparisons are shown in Fig. 8, where the variations of F_f and F_p as functions of the phase speed of the traveling wavy wall, c/U, are shown (F_f is the total friction force, F_p is total pressure force on the wall in the streamwise direction, respectively). Here again our data are in good agreement with the reference simulation [4].

4.2.2. Transitional flow past a mechanical heart valve with moving leaflets

To further demonstrate the capabilities of the present method in handling realistic turbulent and transitional flow problems that involve complex three-dimensional bound-

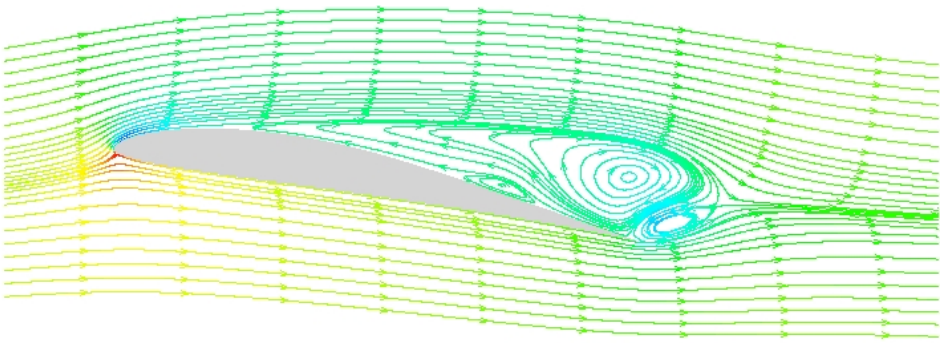

Figure 6. Mean streamlines of an E387 airfoil at attack angle 10° for $Re = 10,000$.

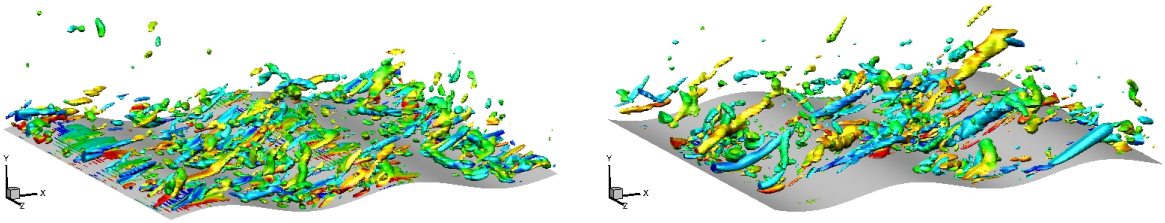

(a) $c/U = 0.0$ (b) $c/U = 0.4$

Figure 7. Instantaneous vortical structures visualized using isosurfaces of $Q = 8.0$ colored by the streamwise vorticity.

aries consisting of multiple moving parts, we have computed the flow past a mechanical bileaflet, heart valve in the aortic position. The shape and size of the leaflets roughly mimics the St. Jude Medical (SJM) Standard bi-leaflet, which is commonly used in clinical practice. The movement of the leaflets is prescribed according to a simplified law that resembles the real movement of the leaflets as determined by their interaction with the blood flow. The configuration which involves the interaction of the flow with a stationary (the aortic chamber) and two moving (the leaflets) boundaries is a great challenge for any structured or unstructured boundary-conforming method. In the present computation the overall geometry is immersed into a Cartesian grid and the boundary conditions on the stationary and moving boundaries are imposed using the method described in the previous sections. The Reynolds number is 4000 based on the peak systole velocity and the artery diameter, which is in the range of practical operation. The computational grid involves $420 \times 200 \times 200$ nodes in streamwise, spanwise (direction parallel to the rotation axis of the leaflets), and transverse directions, respectively. The total number of nodes in this computation is 16.8 million.

The flow in the proximal area of the leaflets is very complicated, and it is dominated

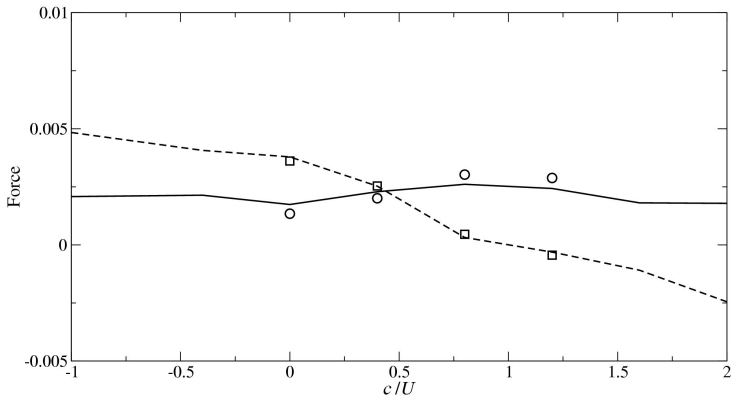

Figure 8. Mean force acting on the traveling wavy boundary as a function of c/U. solid line and circle is total friction force, F_f; dash line and square is the total pressure force, F_p. Lines are the DNS results in [4], and symbols are the present results.

by intricate vortex-leaflet and vortex-vortex interactions. The present method can accurately capture the thin shear layers that form on both moving and stationary immersed boundaries.

To better illuminated the highly three-dimensional nature of the complex vortex interactions just downstream of the leaflets, isosurfaces of Q are shown in Fig 9. Two consecutive instantaneous realizations have been selected ($t/T = 0.7$ and $t/T = 0.8$) which correspond to instances in time near the end of the opening of the valve. In Fig 9a the early stage of the formation of a ring vortex at the expansion plane (structure A) can be seen. At the same time the motion of the leaflets also generate another strong vortex (structure B). At a later time (Fig 9b) both structures evolve and interact with each other and the surrounding flow giving rise to the complex vortex dipoles.

The computation of the flow around the heart valve for example, has been performed on a Linux desktop workstation equipped with four AMD Opteron 846 2GHz processors (each with 1M cache, and 8GB memory in total) takes about 6 CPU hours for one pulsatile cycle. A 10 cycle simulation which with 17 million points can be completed in less than 3 days. For a variety of problems, especially from biology where only low/moderate Reynolds numbers are encountered methods such the present one have a lot of advantages.

5. CONCLUSIONS

REFERENCES

1. E. Balaras, Modeling complex boundaries using an external force field on fixed Cartesian grids in large-eddy simulations. Computers & Fluids, 33 (2004):375–404.
2. T. A. Johnson and V. C. Patel, Flow past a sphere up to a Reynolds number of 300. J. Fluid Mech. 378 (1999):353–385.
3. C. Meneveau, C. S. Lund, and W. H. Cabot, A Lagrangian dynamic subgrid-scale

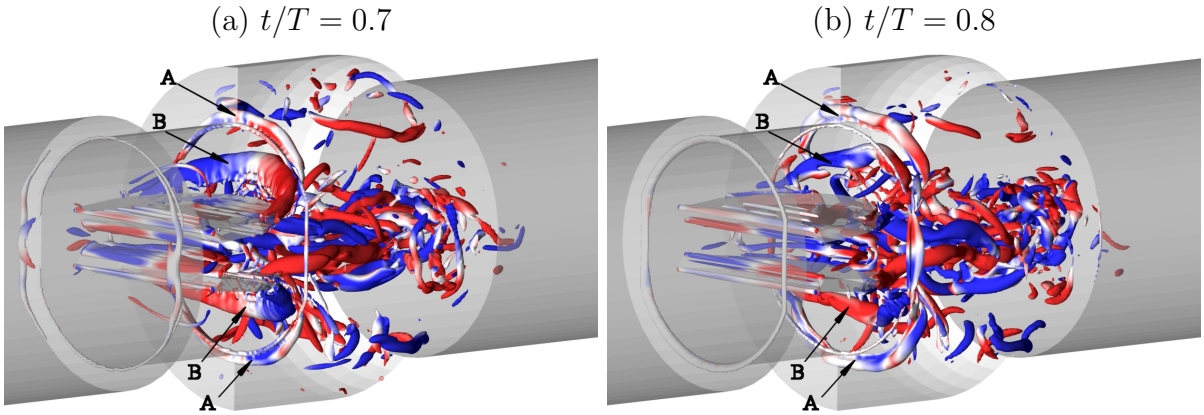

Figure 9. Instantaneous vortical structures visualized using isosurfaces of $Q = 80$ colored by the streamwise vorticity.

model of turbulence. J. Fluid Mech. 319 (1996):353–385.

4. L. Shen, X. Zhang, D. K. P. Yue, and M. S. Triantafyllou, Turbulent flow over a flexible wall undergoing a streamwise travelling wave motion. J. Fluid Mech. 484 (2003):197–221.
5. P.N. Swartzrauber, Direct method for the discrete solution of separable elliptic equations. SIAM J. Num. Anal., 11 (1974):1136–.
6. A. G. Tomboulides and S. A.Orszag, Numerical investigation of transitional and weak turbulent flow past a sphere. J. Fluid Mech. 416 (2000):45–73.
7. J. Yang and E. Balaras, An embedded-boundary formulation for large-eddy simulation of turbulent flows interacting with moving boundaries. J. Comput. Phys., (2005) in review.